Nano Research
2019, 12(7): 1691–1695

ISSN 1998-0124 CN 11-5974/O4
https://doi.org/10.1007/s12274-019-2424-6

Research Article

Thickness determination of MoS_2, $MoSe_2$, WS_2 and WSe_2 on transparent stamps used for deterministic transfer of 2D materials

Najme S. Taghavi[1,2], Patricia Gant[1] (✉), Peng Huang[1,3], Iris Niehues[4], Robert Schmidt[4], Steffen Michaelis de Vasconcellos[4], Rudolf Bratschitsch[4], Mar García-Hernández[1], Riccardo Frisenda[1] (✉), and Andres Castellanos-Gomez[1] (✉)

[1] *Materials Science Factory, Instituto de Ciencia de Materiales de Madrid (ICMM), Consejo Superior de Investigaciones Científicas (CSIC), Sor Juana Inés de la Cruz 3, 28049 Madrid, Spain*
[2] *Faculty of Physics, Khaje Nasir Toosi University of Technology (KNTU), Tehrān 19697 64499, Iran*
[3] *State Key Laboratory of Tribology, Tsinghua University, Beijing 100084, China*
[4] *Institute of Physics and Center for Nanotechnology, University of Münster, 48149 Münster, Germany*

Received: 4 December 2018 / **Revised:** 3 April 2019 / **Accepted:** 27 April 2019

ABSTRACT

Here, we propose a method to determine the thickness of the most common transition metal dichalcogenides (TMDCs) placed on the surface of transparent stamps, used for the deterministic placement of two-dimensional materials, by analyzing the red, green and blue channels of transmission-mode optical microscopy images of the samples. In particular, the blue channel transmittance shows a large and monotonic thickness dependence, making it a very convenient probe of the flake thickness. The method proves to be robust given the small flake-to-flake variation and the insensitivity to doping changes of MoS_2. We also tested the method for $MoSe_2$, WS_2 and WSe_2. These results provide a reference guide to identify the number of layers of this family of materials on transparent substrates only using optical microscopy.

KEYWORDS

transition metal dichalcogenides, optical identification, transparent substrate, trasmittance

1 Introduction

Since the isolation of graphene in 2004 [1], the mechanical exfoliation method (also called Scotch tape method) has established itself as one of the most used techniques to produce two-dimensional (2D) materials [2–5]. Its facile implementation combined with the high quality of the produced samples are most likely the reasons behind the success of this technique. Mechanical exfoliation, nonetheless, yields randomly distributed flakes of various thicknesses and sizes on the surface of the substrate. This limitation has been overcome to a great extent through the development of rapid methods to find and identify thin flakes based on the observation of the apparent color when they are transferred onto a SiO_2/Si surface [6–12]. On this substrate, there is a dependency of the apparent color of the flake with its thickness due to thin-film interference effects and many epi-illumination (reflection mode) microscopy-based methods have been developed to identify 2D materials and to determine their number of layers [6–12]. An alternative way to overcome the limitations of mechanical exfoliation relies on the use of experimental tools that allow for the deterministic placement of flakes onto any desired sample position with micrometer accuracy [13–19]. These transfer techniques opened the field of van der Waals heterostructures [18, 20–23]. To carry out the deterministic placement, the isolated flakes have to be deposited onto the surface of a polymer-based stamp that is used as a release layer or sacrificial carrier substrate. These stamps are made of transparent material to allow for the accurate alignment of the flake to be transferred with the acceptor surface by inspection with an optical microscope. Unfortunately, on the surface of the transparent stamps most of the previously developed optical identification methods, based on the apparent colors, are less straightforward to implement and less effective and other complementary techniques such as Raman or photoluminescence (which are slower and more complex than simple optical microscopy) are typically used to determine the number of layers of the flakes deposited on the polymeric stamps [24–27]. Due to the increasing interest on the use of deterministic placement methods to assemble nanodevices and van der Waals heterostructures, the development of alternative methods to determine the thickness of 2D materials on the surface of the transparent polymeric stamps is extremely relevant for the 2D community. That is exactly the goal of this work, to provide a fast and reliable method to identify transition metal dichalcogenide (TMDC) flakes on transparent polymeric stamps and to determine their number of layers.

Here, we demonstrate that the quantitative analysis of transmission optical mode images of TMDC flakes on the surface of transparent polydimethylsiloxane (PDMS) stamps is a reliable method to accurately determine their thickness. We compare the results of the quantitative analysis of the transmission mode optical images with results obtained via micro-reflectance spectroscopy [28], photoluminescence and Raman spectroscopy to verify its reliability. In order to test the limitations of this method, we probe its sensitivity concerning the doping level of the sample by measuring MoS_2 samples with different intentional doping. We found that the determination of the thickness with the analysis of transmission mode images is rather independent

Address correspondence to Patricia Gant, patricia.gant@csic.es; Riccardo Frisenda, riccardo.frisenda@csic.es; Andres Castellanos-Gomez, andres.castellanos@csic.es

on the doping level, giving similar results for all the studied samples. Finally, we extended the study to other TMDCs to provide a reference guide to identify the number of layers of this family of materials. As the measurement of the transmittance is a differential measurement, the effect of the substrate is accounted for and thus these results could be extrapolated to other transparent stamp surfaces like poly(methyl methacrylate) (PMMA) or polycarbonate/hexagonal boron-nitride (PC/hBN).

2 Results and discussion

Figure 1(a) shows a transmission mode optical microscopy image of a MoS_2 flake transferred onto a Gel-Film substrate (a commercially available polydimethylsiloxane film, by Gel-Pak) which is typically used as a stamp for deterministic dry transfer of 2D materials [16, 29]. Figure 1(b) displays line profiles of the intensity of the red, green and blue (RGB) channels extracted from the image in Fig. 1(a). The transmittance of the different channels is calculated by normalizing the RGB channel images to the intensity of these channels measured on the bare substrate. From the line profiles, one can see that the transmittance of each channel changes stepwise with the number of layers. To determine the feasibility of using the transmittance to determine the number of layers one needs to characterize the statistical variations of the transmittance in different MoS_2 flakes and the uncertainty associated to these measurements. Therefore, we acquired transmission mode optical microscopy images of 202 MoS_2 flakes and we compiled three histograms by binning the measured transmittance of the flakes for each color channel. Figure 1(c) shows the histograms of the RGB channels plotted versus 1-transmittance. Although all the histograms display prominent peaks that correspond to different number of layers, the histogram of the blue channel shows a larger separation between the peaks (while maintaining a similar peak width) making it easier to distinguish between 1, 2, 3 or 4 layers of MoS_2. The higher contrast of the blue channel is expected as MoS_2 (and $MoSe_2$, WS_2 and WSe_2 as well) present a strong excitonic feature (sometimes referred to as C exciton in the literature) in the blue part of the spectrum that yields a strong optical absorption in that wavelength range [30, 31].

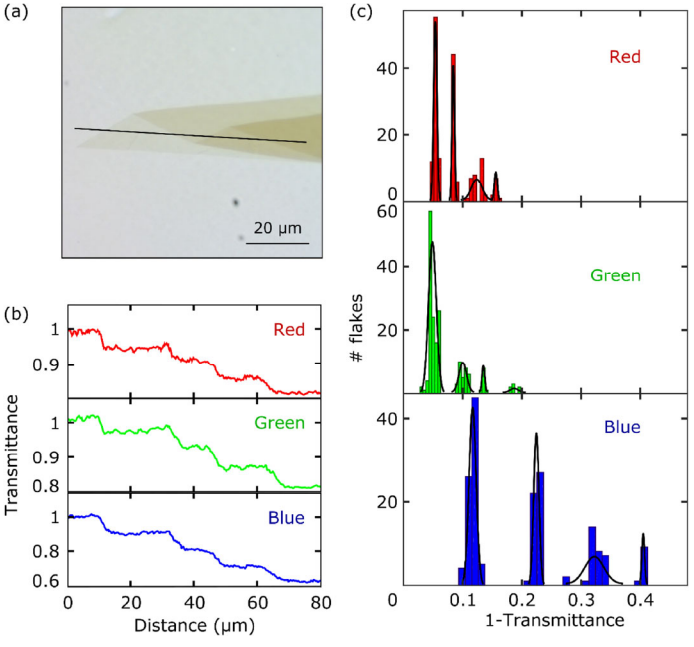

Figure 1 (a) Optical image in transmission mode of a MoS_2 flake with different thicknesses. (b) Line profiles of the intensities of the RGB channels of the image in (a). (c) Histograms of the 1-transmission value in the RGB channels for several MoS_2 flakes.

In order to verify the reliability of this method to determine the number of layers we benchmarked it with other commonly used spectroscopic techniques. In Fig. 2(a) the experimental data employed to build up the histogram in Fig. 1(c) is displayed in a scatter plot. We have selected 4 flakes with different thickness in the range between 1 layer and 4 layers, respectively, labeled as 1L, 2L, 3L and 4L accordingly to their blue channel transmission, and we have carried out micro-reflection, Raman and photoluminescence measurements to have three independent methods to determine the thickness. Figure 2(b) shows the differential reflectance spectra acquired on these flakes where the intensity and the energy of the A exciton monotonically changes from 1L to 4L. The intensities and exciton positions obtained in the spectra agree with the values expected for 1L to 4L [31], which means a correct assignment of the thickness estimated by the blue channel values [32]. Figure 2(c) compares the Raman spectra measured on the same flakes (vertically displaced by 0.1 for clarity) with a 532 nm excitation laser. We verify the number of layers of the samples from the difference between the A_{1g} and E^1_{2g} phonon [33, 34] energies in Raman and check again the accuracy in the determination of the number of layers using the blue channel transmittance. Figure 2(d) shows photoluminescence measurements for 1L, 2L, 3L and 4L flakes, also measured with a 532 nm excitation laser. The intensity and the position of the A exciton dramatically depends on the number of layers and it confirms that the assignment of number of layers determined by the blue channel transmission is reliable [24, 35].

We further test the analysis of the blue channel transmission images by studying MoS_2 samples synthesized with intentional substitutional metal atoms at the Mo sites to enquiry about the robustness of this technique against a moderate variation of the chemical composition that lead to a big change in the electronic properties [36, 37]. We follow the synthesis method described in Refs. [36–39] for the growth of Fe-doped, Ni-doped, Nb-doped and Co-doped MoS_2 crystals. In all cases a 0.5% of dopant material has been added in the ampoule for the synthesis of these doped MoS_2 samples which lead to a final doping level in the 0.3%–0.4% range.

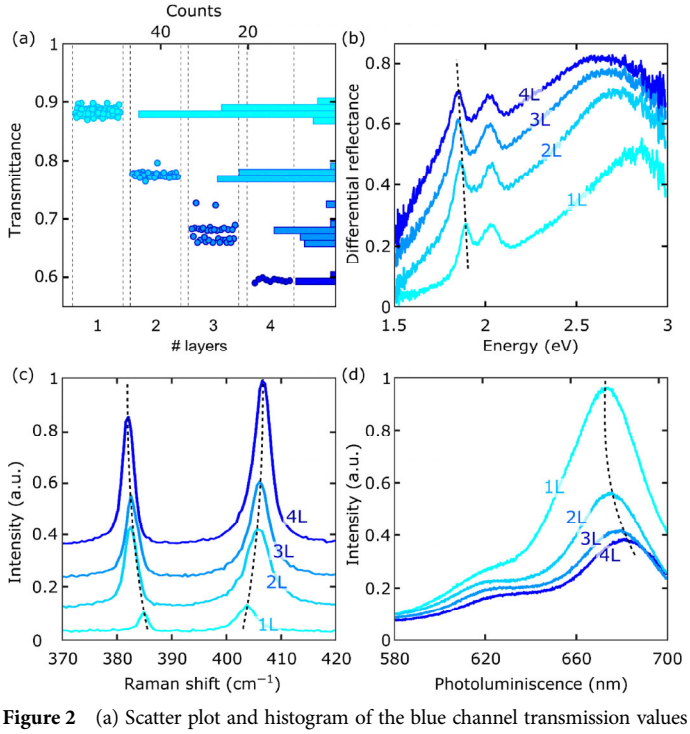

Figure 2 (a) Scatter plot and histogram of the blue channel transmission values for several MoS_2 flakes. (b) Differential reflectance spectra for MoS_2 with different number of layers. (c) Raman spectra for MoS_2 with different number of layers. (d) Photoluminescence of MoS_2 for different number of layers.

Figure 3 compares the histograms of the blue channel transmittance constructed by analyzing 50 flakes of each doped MoS_2 material. This comparison clearly illustrates how our method is rather insensitive to variations of the chemical composition (that induces strong changes in the doping level of the material). We note that other optical spectroscopic methods to determine the thickness of transition metal dichalcogenides such as Raman and photoluminescence spectroscopy are strongly dependent on the doping level of the samples and on slight variations of the chemical composition [40–44].

We extended this method to other 2D materials of the TMDCs family to provide a general guide to identify these materials through the analysis of the blue channel of transmission images. Figure 4 compares the blue channel transmission histograms built up after analyzing 202 MoS_2 flakes, 200 $MoSe_2$ flakes, 200 WS_2 flakes and 200 WSe_2 flakes. In all the cases the histograms show well-resolved peaks indicating that one can unambiguously determine the number of layers through the quantitative analysis of the blue channel of the transmission mode optical images.

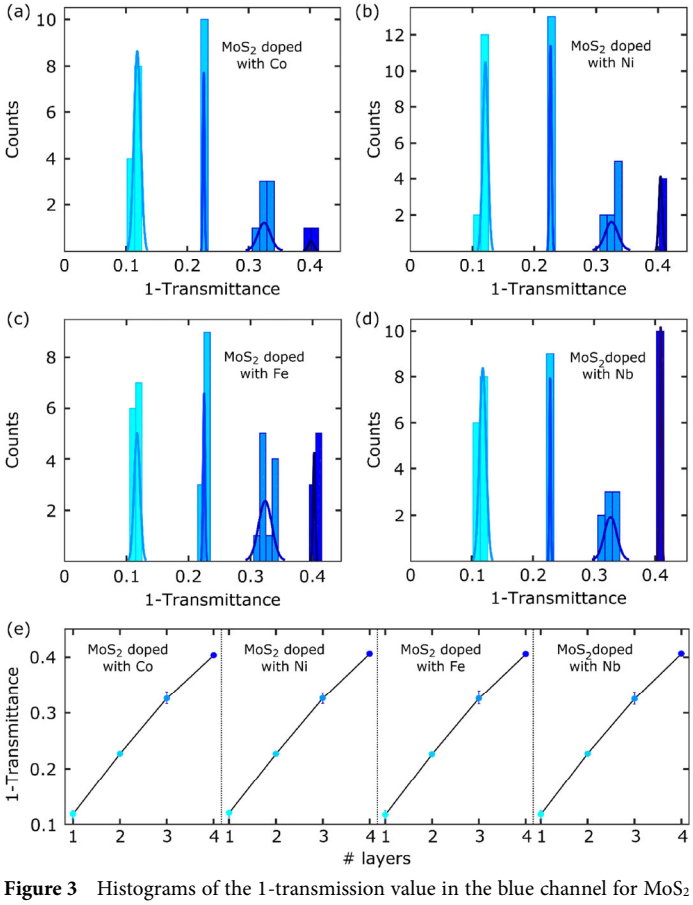

Figure 3 Histograms of the 1-transmission value in the blue channel for MoS_2 flakes doped with (a) Co, (b) Ni, (c) Fe and (d) Nb. (e) Average of the 1-transmission values for 1L to 4L in each material.

3 Conclusions

In summary, we have introduced a very simple and fast yet reliable method to determine the number of layers of MoS_2, $MoSe_2$, WS_2 and WSe_2 deposited on a PDMS stamp, used for deterministic placement of 2D materials. Moreover, being a differential measurement, the effect of the substrate is removed and it could be extended to other transparent substrates. We have demonstrated that the transmittance, extracted from the blue channel of transmission mode optical images, monotonically depends on the number of layers. We have benchmarked the layer assignment done with this method with other extended spectroscopic techniques (micro-reflection, Raman, photoluminescence) finding an excellent agreement. Interestingly, this method is robust enough to provide an accurate layer determination even for samples with different doping level. In view of all this, the quantitative analysis of the transmission mode images can become a powerful method to select the flakes of 2D materials deposited onto transparent polymeric stamps prior to their deterministic transfer.

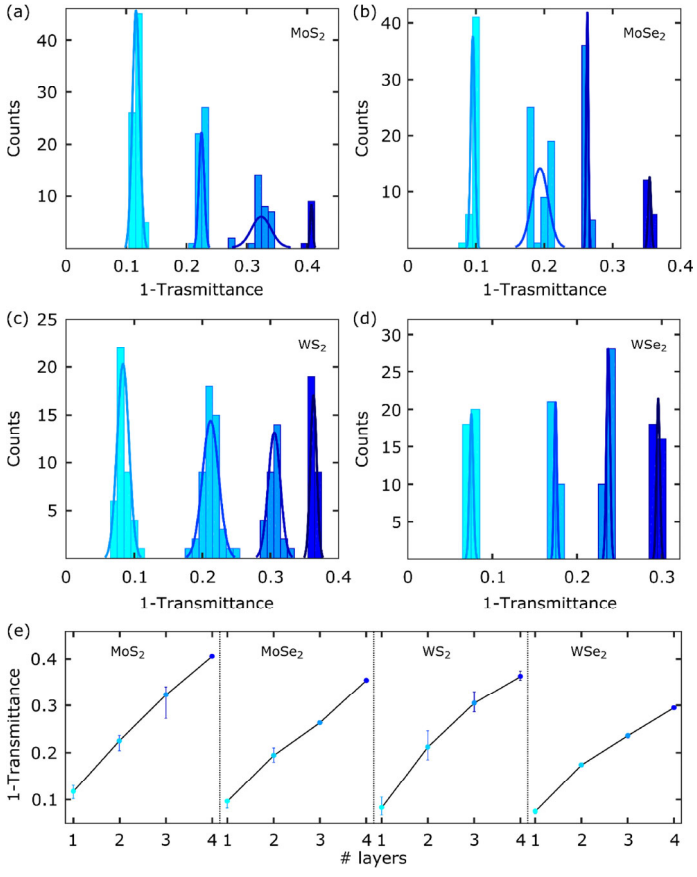

Figure 4 Histograms of the 1-transmittance value in the blue channel for (a) MoS_2, (b) $MoSe_2$, (c) WS_2 and (d) WSe_2 flakes. (e) Average of the 1-transmittance values for 1L to 4L in each material.

4 Experimental

4.1 Materials

MoS_2 samples were prepared out of a bulk natural molybdenite crystal (Moly Hill mine, Quebec, Canada). $MoSe_2$ and WSe_2 samples were prepared out of bulk synthetic crystals grown by physical vapour transport method (provided by Prof. Rudolf Bratschitsch). WS_2 samples were prepared out of a bulk synthetic crystal grown by physical vapour transport method at Tennessee Crystal Center. The Fe-doped, Ni-doped, Nb-doped and Co-doped MoS_2 crystals (provided by Prof. Der-Yuh Lin and Prof. Tsung-Shine Ko) were grown following the protocols described in Refs. [36–39]. A 0.5% of dopant material has been added during the synthesis of these doped MoS_2 samples which leads to a final doping level in the 0.3%–0.4% range.

The transparent stamp substrate used in this work is a commercially available polydimethylsiloxane-based substrate manufactured by Gel-Pak® (Gel-Film® WF X4 6.0 mil). The TMDC flakes are exfoliated from the bulk crystals and transferred onto the surface of the Gel-Film stamp with a Nitto 224SPV adhesive tape.

4.2 Optical microscopy

Optical microscopy images have been acquired with three different upright metallurgical microscopes, an AM Scope, a Motic BA

MET310-T and a Nikon Eclipse CI, obtaining identical results. The transmission mode images have been acquired with an achromat condenser lens (N.A. 0.85) that ensures Köhler illumination, yielding to a homogeneous illumination spot of approximately 4 mm^2 on the sample. The light was collected with a 50× magnification plan achromatic objective (NA 0.55). Two different digital cameras were tested during this work, an AM Scope mu1803 camera with 18 megapixels and a Canon EOS 1200D, also providing identical results.

4.3 Image analysis

The quantitative analysis of the transmittance of the flakes and the rippling wavelength has been carried out using Gwyddion® and ImageJ software [45, 46].

Acknowledgements

We thank Prof. Der-Yuh Lin and Prof. Tsung-Shine Ko for providing the doped MoS_2 samples. N. S. T. acknowledges to the Ministry of Science, Research and Technology of Iran. A. C. G. and P. G. acknowledge funding from the European Commission Graphene Flagship (Grant Graphene Core 2 785219). R. F. acknowledges support from the Netherlands Organization for Scientific Research (NWO) through the research program Rubicon with project number 680-50-1515. A. C. G. acknowledge funding from the European Research Council (ERC) under the European Union's Horizon 2020 research and innovation programme (grant agreement n° 755655, ERC-StG 2017 project 2D-TOPSENSE).

Electronic Supplementary Material: Supplementary material (constructing a thickness map from a transmission mode optical microscopy image and blue channel transmittance measurements for flakes thicker than 4 layers) is available in the online version of this article at https://doi.org/10.1007/s12274-019-2424-6.

References

[1] Novoselov, K. S.; Geim, A. K.; Morozov, S. V; Jiang, D.; Zhang, Y.; Dubonos, S. V; Grigorieva, I. V; Firsov, A. A. Electric field effect in atomically thin carbon films. *Science* **2004**, *306*, 666–669.

[2] Bonaccorso, F.; Lombardo, A.; Hasan, T.; Sun, Z. P.; Colombo, L.; Ferrari, A. C. Production and processing of graphene and 2D crystals. *Mater. Today* **2012**, *15*, 564–589.

[3] Ferrari, A. C.; Bonaccorso, F.; Fal'ko, V.; Novoselov, K. S.; Roche, S.; Bøggild, P.; Borini, S.; Koppens, F. H. L.; Palermo, V.; Pugno, N. et al. Science and technology roadmap for graphene, related two-dimensional crystals, and hybrid systems. *Nanoscale* **2015**, *7*, 4598–4810.

[4] Radisavljevic, B.; Radenovic, A.; Brivio, J.; Giacometti, V.; Kis, A. Single-layer MoS_2 transistors. *Nat. Nanotechnol.* **2011**, *6*, 147–150.

[5] Wang, Q. H.; Kalantar-Zadeh, K.; Kis, A.; Coleman, J. N.; Strano, M. S. Electronics and optoelectronics of two-dimensional transition metal dichalcogenides. *Nat. Nanotechnol.* **2012**, *7*, 699–712.

[6] Ni, Z. H.; Wang, H. M.; Kasim, J.; Fan, H. M.; Yu, T.; Wu, Y. H.; Feng, Y. P.; Shen, Z. X. Graphene thickness determination using reflection and contrast spectroscopy. *Nano Lett.* **2007**, *7*, 2758–2763.

[7] Jung, I.; Pelton. M.; Piner, R.; Dikin, D. A.; Stankovich, S.; Watcharotone, S.; Hausner, M.; Ruoff, R. S. Simple approach for high-contrast optical imaging and characterization of graphene-based sheets. *Nano Lett.* **2007**, *7*, 3569–3575.

[8] Li, H.; Wu, J.; Huang, X.; Lu, G.; Yang, J.; Lu, X.; Xiong, Q. H.; Zhang, H. Rapid and reliable thickness identification of two-dimensional nanosheets using optical microscopy. *ACS Nano* **2013**, *7*, 10344–10353.

[9] Wang, X. F.; Zhao, M.; Nolte, D. D. Optical contrast and clarity of graphene on an arbitrary substrate. *Appl. Phys. Lett.* **2009**, *95*, 081102.

[10] Zhang, H.; Ran, F. R.; Shi, X. T.; Fang, X. R.; Wu, S. Y.; Liu, Y.; Zheng, X. Q.; Yang, P.; Liu, Y.; Wang, L. et al. Optical thickness identification of transition metal dichalcogenide nanosheets on transparent substrates. *Nanotechnology* **2017**, *28*, 164001.

[11] Yu, Y. F.; Li, Z. Z.; Wang, W. H.; Guo, X. T.; Jiang, J.; Nan, H. Y.; Ni, Z. H. Investigation of multilayer domains in large-scale CVD monolayer graphene by optical imaging. *J. Semicond.* **2017**, *38*, 033003.

[12] Wang, Y. Y.; Gao, R. X.; Ni, Z. H.; He, H.; Guo, S. P.; Yang, H. P.; Cong, C. X.; Yu, T. Thickness identification of two-dimensional materials by optical imaging. *Nanotechnology* **2012**, *23*, 495713.

[13] Dean, C. R.; Young, A. F.; Meric, I.; Lee, C.; Wang, L.; Sorgenfrei, S.; Watanabe, K.; Taniguchi, T.; Kim, P.; Shepard, K. L. et al. Boron nitride substrates for high-quality graphene electronics. *Nat. Nanotechnol.* **2010**, *5*, 722–726.

[14] Zomer, P. J.; Dash, S. P.; Tombros, N.; van Wees, B. J. A transfer technique for high mobility graphene devices on commercially available hexagonal boron nitride. *Appl. Phys. Lett.* **2011**, *99*, 232104.

[15] Zomer, P. J.; Guimarães, M. H. D.; Brant, J. C.; Tombros, N.; van Wees, B. J. Fast pick up technique for high quality heterostructures of bilayer graphene and hexagonal boron nitride. *Appl. Phys. Lett.* **2014**, *105*, 013101.

[16] Castellanos-Gomez, A.; Buscema, M.; Molenaar, R.; Singh, V.; Janssen, L.; van der Zant, H. S. J.; Steele, G. A. Deterministic transfer of two-dimensional materials by all-dry viscoelastic stamping. *2D Mater.* **2014**, *1*, 011002.

[17] Pizzocchero, F.; Gammelgaard, L.; Jessen, B. S.; Caridad, J. M.; Wang, L.; Hone, J.; Bøggild, P.; Booth, T. J. The hot pick-up technique for batch assembly of van der Waals heterostructures. *Nat. Commun.* **2016**, *7*, 11894.

[18] Frisenda, R.; Navarro-Moratalla, E.; Gant, P.; de Lara, D. P.; Jarillo-Herrero, P.; Gorbachev, R. V; Castellanos-Gomez, A. Recent progress in the assembly of nanodevices and van der Waals heterostructures by deterministic placement of 2D materials. *Chem. Soc. Rev.* **2018**, *47*, 53–68.

[19] Masubuchi, S.; Morimoto, M.; Morikawa, S.; Onodera, M.; Asakawa, Y.; Watanabe, K.; Taniguchi, T.; Machida, T. Autonomous robotic searching and assembly of two-dimensional crystals to build van der Waals superlattices. *Nat. Commun.* **2018**, *9*, 1413.

[20] Liu, Y.; Weiss, N. O.; Duan, X. D.; Cheng, H. C.; Huang, Y.; Duan, X. F. Van der Waals heterostructures and devices. *Nat. Rev. Mater.* **2016**, *1*, 16042.

[21] Geim, A. K.; Grigorieva, I. V. Van der Waals heterostructures. *Nature* **2013**, *499*, 419–425.

[22] Novoselov, K. S.; Mishchenko, A.; Carvalho, A.; Castro Neto, A. H. 2D materials and van der Waals heterostructures. *Science* **2016**, *353*, aac9439.

[23] Frisenda, R.; Molina-Mendoza, A. J.; Mueller, T.; Castellanos-Gomez, A.; van der Zant, H. S. J. Atomically thin p–n junctions based on two-dimensional materials. *Chem. Soc. Rev.* **2018**, *47*, 3339–3358.

[24] Splendiani, A.; Sun, L.; Zhang, Y. B.; Li, T. S.; Kim, J.; Chim, C. Y.; Galli, G.; Wang, F. Emerging photoluminescence in monolayer MoS_2. *Nano Lett.* **2010**, *10*, 1271–1275.

[25] Pimenta, M. A.; del Corro, E.; Carvalho, B. R.; Fantini, C.; Malard, L. M. Comparative study of Raman spectroscopy in graphene and MoS_2-type transition metal dichalcogenides. *Acc. Chem. Res.* **2015**, *48*, 41–47.

[26] Zhang, X.; Qiao, X. F.; Shi, W.; Wu, J. B.; Jiang, D. S.; Tan, P. H. Phonon and Raman scattering of two-dimensional transition metal dichalcogenides from monolayer, multilayer to bulk material. *Chem. Soc. Rev.* **2015**, *44*, 2757–2785.

[27] Zeng, H. L.; Cui, X. D. An optical spectroscopic study on two-dimensional group-VI transition metal dichalcogenides. *Chem. Soc. Rev.* **2015**, *44*, 2629–2642.

[28] Frisenda, R.; Niu, Y.; Gant, P.; Molina-Mendoza, A. J.; Schmidt, R.; Bratschitsch, R.; Liu, J. X.; Fu, L.; Dumcenco, D.; Kis, A. et al. Micro-reflectance and transmittance spectroscopy: A versatile and powerful tool to characterize 2D materials. *J. Phys. D Appl. Phys.* **2017**, *50*, 074002.

[29] Yang, R.; Zheng, X. Q.; Wang, Z. H.; Miller, C. J.; Feng, P. X. L. Multilayer MoS_2 transistors enabled by a facile dry-transfer technique and thermal annealing. *J. Vac. Sci. Technol. B* **2014**, *32*, 061203.

[30] Castellanos-Gomez, A.; Quereda, J.; van der Meulen, H. P.; Agraït, N.; Rubio-Bollinger, G. Spatially resolved optical absorption spectroscopy of single- and few-layer MoS_2 by hyperspectral imaging. *Nanotechnology* **2016**, *27*, 115705.

[31] Niu, Y.; Gonzalez-Abad, S.; Frisenda, R.; Marauhn, P.; Drüppel, M.; Gant, P.; Schmidt, R.; Taghavi, N. S.; Barcons, D.; Molina-Mendoza, A. J. et al. Thickness-dependent differential reflectance spectra of monolayer and few-layer MoS_2, $MoSe_2$, WS_2 and WSe_2. *Nanomaterials* **2018**, *8*, 725.

[32] Li, H.; Zhang, Q.; Yap, C. C. R.; Tay, B. K.; Edwin, T. H. T.; Olivier, A.; Baillargeat, D. From bulk to monolayer MoS_2: Evolution of Raman scattering. *Adv. Funct. Mater.* **2012**, *22*, 1385–1390.

[33] Lee, C.; Yan, H. G.; Brus, L. E.; Heinz, T. F.; Hone, J.; Ryu, S. Anomalous lattice vibrations of single- and few-layer MoS_2. *ACS Nano* **2010**, *4*, 2695–2700.
[34] Tonndorf, P.; Schmidt, R.; Böttger, P.; Zhang, X.; Börner, J.; Liebig, A.; Albrecht, M.; Kloc, C.; Gordan, O.; Zahn, D. R. T. et al. Photoluminescence emission and Raman response of monolayer MoS_2, $MoSe_2$, and WSe_2. *Opt. Express* **2013**, *21*, 4908–4916.
[35] Mak, K. F.; Lee, C.; Hone, J.; Shan, J.; Heinz, T. F. Atomically thin MoS_2: A new direct-gap semiconductor. *Phys. Rev. Lett.* **2010**, *105*, 136805.
[36] Suh, J.; Park, T. E.; Lin, D. Y.; Fu, D. Y.; Park, J.; Jung, H. J.; Chen, Y. B.; Ko, C.; Jang, C.; Sun, Y. H. et al. Doping against the native propensity of MoS_2: Degenerate hole doping by cation substitution. *Nano Lett.* **2014**, *14*, 6976–6982.
[37] Svatek, S. A.; Antolin, E.; Lin, D. Y.; Frisenda, R.; Reuter, C.; Molina-Mendoza, A. J.; Muñoz, M.; Agraït, N.; Ko, T. S.; de Lara, D. P. et al. Gate tunable photovoltaic effect in MoS_2 vertical p–n homostructures. *J. Mater. Chem. C* **2017**, *5*, 854–861.
[38] Reuter, C.; Frisenda, R.; Lin, D. Y.; Ko, T. S.; Perez de Lara, D.; Castellanos-Gomez, A. A versatile scanning photocurrent mapping system to characterize optoelectronic devices based on 2D materials. *Small Methods* **2017**, *1*, 1700119.
[39] Wang, S. Y.; Ko, T. S.; Huang, C. C.; Lin, D. Y.; Huang, Y. S. Optical and electrical properties of MoS_2 and Fe-doped MoS_2. *Jpn. J. Appl. Phys.* **2014**, *53*, 04EH07.
[40] Chen, Y. F.; Dumcenco, D. O.; Zhu, Y. M.; Zhang, X.; Mao, N. N.; Feng, Q. L.; Zhang, M.; Zhang, J.; Tan, P. H.; Huang, Y. S. et al. Composition-dependent Raman modes of $Mo_{1-x}W_xS_2$ monolayer alloys. *Nanoscale* **2014**, *6*, 2833–2839.
[41] Dumcenco, D. O.; Kobayashi, H.; Liu, Z.; Huang, Y. S.; Suenaga, K. Visualization and quantification of transition metal atomic mixing in $Mo_{1-x}W_xS_2$ single layers. *Nat. Commun.* **2013**, *4*, 1351.
[42] Mann, J.; Ma, Q.; Odenthal, P. M.; Isarraraz, M.; Le, D.; Preciado, E.; Barroso, D.; Yamaguchi, K.; von Son Palacio, G.; Nguyen, A. et al. 2-Dimensional transition metal dichalcogenides with tunable direct band gaps: $MoS_{2(1-x)}Se_{2x}$ monolayers. *Adv. Mater.* **2014**, *26*, 1399–1404.
[43] Zhang, M.; Wu, J. X.; Zhu, Y. M.; Dumcenco, D. O.; Hong, J. H.; Mao, N. N.; Deng, S. B.; Chen, Y. F.; Yang, Y. L.; Jin, C. H. et al. Two-dimensional molybdenum tungsten diselenide alloys: Photoluminescence, Raman scattering, and electrical transport. *ACS Nano* **2014**, *8*, 7130–7137.
[44] Mouri, S.; Miyauchi, Y.; Matsuda, K. Tunable photoluminescence of monolayer MoS_2 via chemical doping. *Nano Lett.* **2013**, *13*, 5944–5948.
[45] Nečas, D.; Klapetek, P. Gwyddion: An open-source software for SPM data analysis. *Open Phys.* **2012**, *10*, 181–188.
[46] Abràmoff, M. D.; Magalhães, P. J.; Ram, S. J. Image processing with imageJ. *Biophotonics Int.* **2004**, *11*, 36–42.